USE OF BCN TEST FOR CONTROLLING TENSION CAPACITY OF FIBER REINFORCED SHOTCRETE IN MINING WORKS

SERGIO CARMONA[1]

Departamento de Obras Civiles, Universidad Técnica Federico Santa María

Valparaíso, Chile

and

CLIMENT MOLINS

Departamento de Ingeniería Civil y Ambiental

Universitat Politècnica de Catalunya,

Barcelona, España

ABSTRACT

Fiber reinforced shotcrete (FRS) is widely used for tunnel construction. However, the systematic control of FRS properties is hampered by the complexities of the experimental procedures used. The experiments are normally based on the load-deflection response obtained from flexural tests with third-point loading performed under displacement control. These types of tests are characterized by instability when the cracking load is reached and, subsequently, errors occur in the deflection measurements, increasing the dispersion of the results. An alternative test, the Barcelona test, has some experimental advantages for FRS control as the use of much smaller specimens, an easy procedure and a lower scatter.

Using the mean crack opening, correlations were established between the Barcelona test and the flexure test to estimate the toughness and residual strengths at a deflection of 3.0 mm. Equivalences between the two tests were obtained based on the laboratory results

[1]Corresponding author: sergio.carmona@usm.cl, Casilla 110- V Valparaíso, Chile. Tel. +56322654382 Fax +56322654115

and were validated based on work site results, with differences of less than 5% of the residual strength.

These relationships and advantages have allowed the Barcelona test to be proposed to control the properties of the FRSs used in the Chuquicamata Underground (Chuquicamata Subterránea) Project developed by the mining company CODELCO-Chile.

KEYWORDS: Third-point bending test, toughness, fiber reinforced shotcrete, BCN test, residual strength.

1. INTRODUCTION

As is widely known, the incorporation of fibers significantly improves the behavior of cracked concrete, which when combined with the operational and safety advantages of spraying, has resulted in fiber reinforced shotcrete (FRS) being widely used for tunneling support in mining projects, roads and hydroelectric plants. One of these applications is the Chuquicamata Underground (*Chuquicamata Subterránea*) Project developed by CODELCO-Chile, where the use of shotcrete reinforced with a electro welded steel mesh with $A_s = 295$ mm^2/m and a yielding stress $f_y = 500$ MPa has been replaced by synthetic fiber reinforced shotcrete for the support of approximately 100 km of tunnels.

For this support, the fiber reinforced shotcrete was designed using parameters defined by ASTM C 1609 (2012) for fiber reinforced concretes (FRC), specifying a flexural residual strength $f_{150}^{D} \geq 2.30$ MPa, and an equivalent flexural strength ratio $R_{T,150}^{D} \geq 62\%$ (Carmona, 2012).

Because the design of this FRS is based on stresses parameters defined at a net deflection δ = 3.0 mm, the quality control of the FRS by three-point bending (3PB) test defined in the standard EN 14651 (CEN, 2005) or the energy absorption capacity determined by testing square panel according to standard EN 14488–5 (CEN, 2006) or recommendation EFNARC (1996), were discarded.

However, the results of four-point bending (4PB) test performed following the ASTM C 1609 standard are characterized by high scatter (Chao *et al*., 2011; Carmona *et al*., 2012) because the beams develop a reduced fracture surface, and the properties directly depend on the specific number of fibers that cross the cracked section; therefore, a representative volume of the material cannot be evaluated. In addition, relatively heavy specimens are required to perform these tests, and the experimental procedures given in the standards are complex, which make these tests inadequate for on-site FRC control.

In this way, the "Barcelona method" proposed by Molins *et al*. (2009) can be used to obtain the FRC residual strength and toughness from the load-total circumferential opening displacement ($TCOD$) response for a cylindrical specimen subjected to a double-punch test (DPT). This method has been standardized in Spain by AENOR (2010) and is characterized by its simplicity of execution and the low dispersion of its results.

Considering the experimental difficulties associated with controlling FRS using the 4PB test outlined in the ASTM C 1609 standard, which is difficult to execute, the objective of this paper is to propose an equivalent method in which the Barcelona (BCN) test can be used to control FRSs in the construction of tunnel supports.

To establish equivalences between both 4PB test and BCN test, which allow performing the quality control of FRS by mean of BCN test, this research was developed at laboratory and real tunnel works levels.

Studies of failure mechanisms and the equivalence between crack openings have resulted in practical correlations among various test methods. First, this article briefly presents a flexural test following the ASTM 1609 standard and the experimental sources of error that affect the determination of FRC properties. Then, an equivalence is developed between the deflection and crack opening of the ASTM beam. The inclusion of the actual eccentricity of the crack in estimating the average crack opening from the deflection of

the beam produced differences of less than 10% with respect to the actual opening recorded during the tests.

Then, this equivalence between the deflection and the crack is further related to the crack opening in a cylinder subjected to a double punch in the Barcelona (BCN) test. Finally, based on the results of experimental three concretes reinforced with 6, 8 and 12 kg/m^3 of synthetic fibers were cast and tested in the laboratory, correlations between toughness and residual strengths obtained with 4PB and BCN tests are proposed for both toughness and residual strength.

It is worth noting that all lab specimens used for deriving the correlation were premix and casted whilst the real tunnel construction specimens came from spraying. Despite the similarity of the mix proportions between these two concretes, their different application produces well-known differences between them (Bjøntegaard *et al*., 2018). This is the reason why the correlation was stablished in-between the premix casted lab samples and, then, the validation was based on panels sprayed in the tunnel. From those panels, ASTM beams and cylindrical cores were cut and prepared for testing. In this way, the significant effects of spraying, such as fiber orientation and porosity, do not intervene in the correlation because it correlates identical concretes.

These correlations are verified using the results of samples obtained in the tunnel construction of the Chuquicamata Underground Project developed by CODELCO-Chile. The results of this research indicate that the properties of the FRSs used in this project can be controlled based on the BCN test.

2. FLEXURAL TEST

Experimentally, the load-deformation response of a specimen under tensile stress is used to determine the properties of FRC. Theoretically, direct tensile test is the most suitable method to determine the specimen properties. However, because this is a difficult test to perform and its results can widely vary (Barragán *et al*., 2003; Cavalaro and Aguado,

2015), in practice, the properties of FRC are often characterized and controlled by the load-crack opening or load-deflection responses obtained by 3PB tests (CEN, 2005) or 4PB tests (EFNARC, 1996; CEN, 2006; ASTM, 2012; ASTM, 2017), respectively.

According to the ASTM C 1609 standard, the residual strength, toughness and equivalent strength of FRC are determined using the load-deflection response obtained by testing a beam subjected to 4PB. For concrete reinforced with fibers between 50 and 75 mm in length, the beam must have a height of 150 mm. This test must be performed in a closed-loop servo - hydraulic system with controlled by the net deflection (δ) measured at the midspan of the beam ($L/2$), at a rate between 0.035 and 0.10 mm/min until a net deflection equal to $L/900$ for beams of dimension $b = h$ =150 mm. After reaching this deflection level, the speed of the net deflection increases in the range of 0.05-0.30 mm/min until the final deflection level. The load (P) and the net deflection (δ) are recorded continuously during the test.

The strength is defined by the first peak, f_1, and the residual strengths f_{600}^D and f_{150}^D, which can be calculated using the loads corresponding to the first peak and deflections of $L/600$ and $L/150$, respectively, with the following expression:

$$f = \frac{P\,L}{bh^2} \tag{1}$$

where P is the load corresponding to the first peak and deflections of $L/600$ and $L/150$, L is the span between the supports, and b and h are the width and height of the beam, respectively.

Additionally, ASTM C 1609 establishes that toughness, T_{150}^D, is calculated as the area under the $P-\delta$ curve from 0 to a net deflection of $\delta = L/150$, which corresponds to $\delta = 3$ mm for beams with $b = h = 150$ mm. For this net deflection, the equivalent flexural strength ratio, $R_{T,150}^D$, is calculated using the following expression:

$$R_{T,150}^D = \frac{150 \cdot T_{150}^D}{f_1 \cdot b \cdot h^2} \cdot 100\ (\%) \tag{2}$$

However, parameters based on the $P - \delta$ response have been widely questioned in the past by Gopalaratnam and Gettu (1995) and Barr *et al.* (1996), who reviewed the limitations of flexural tests with third-point loading to determine FRC properties. Based on these investigations, observations made during the execution of these tests and an analysis of the results, the primary experimental sources of error that affect the determination of FRC properties were identified as follows: (1) due the test setup, theoretically the tensile stress on the central third of beam is constant, therefore cracking begin where cementitious matrix is weakest. Then normally, a crack does not open on the central plane of the beam, which distorts the measurement of the deflection because different deflections can result from the same angle of rotation, as shown in Figure 1a; and (2) according to the standard C 1609, the test must be executed under deflection control in a system with closed-loop control. However, as shown in Figure 1b, when the cracking load is reached, unstable crack propagation occurs because the speed of the crack opening displacement (COD) is greater than the rate of increase of the deflection, which causes a "snap back", as seen in Figure 1c, where the $P - \delta$ and $P - COD$ curves are shown simultaneously until the same time in the test. During the test executed according to the standard, the most important deformation of the test specimen was not controlled. Therefore, in many tests, control is lost until the fibers restrict the opening of the crack, which prevents the softening that the material undergoes after cracking from being adequately measured. This effect is much more sensitive when low quantities of fiber are used, and various researchers have attempted to improve the method by increasing the rigidity of the test systems, i.e., by reducing the rate of deflection during the test or by placing a steel sheet under the specimen, as recommended in ASTM C 1399/1399M-10 (ASTM, 2017).

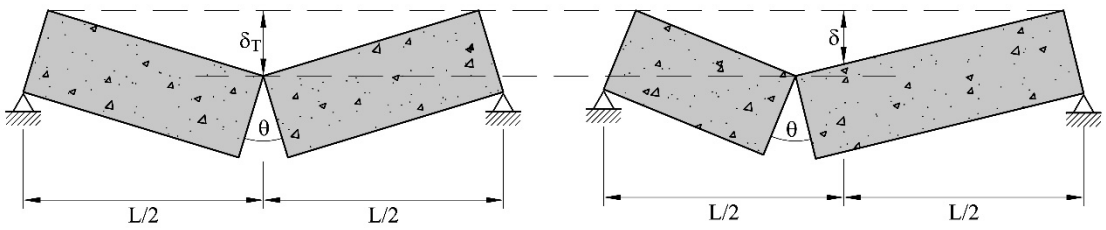

(a)

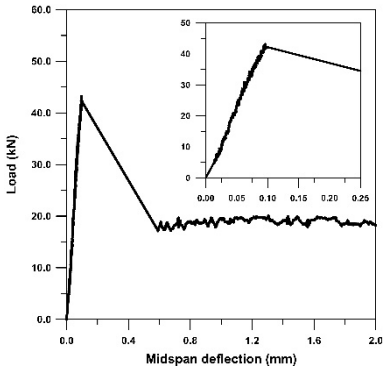

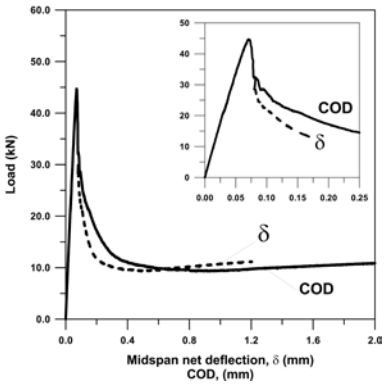

(b) **(c)**

Figure 1. (a) Difference in the measurement of deflection when crack does not open in the midspan plane; (b) $P-\delta$ curve with loss of control during test when the cracking load is reached; (c) $P-\delta$ and $P-COD$ curves at the same time in 4PB test.

3. BARCELONA TEST

According to the UNE 83 515 standard (AENOR, 2010), the Barcelona method, or BCN test, consists of subjecting a cylindrical specimen with diameter (d) and height (H) equal to 150 mm to uniaxial compression using two steel wedges of diameter $a = d/4$, which induces double-punch failure. This test is performed in a conventional testing system under piston displacement control at a rate of 0.5 ± 0.05 mm/min. During the test, the applied load and the circumferential deformation measured at half the height of the specimen must be continuously recorded. When the stress state in the specimen reaches the tensile strength of concrete, cracks open, and the circumferential deformation corresponds to the $TCOD$. The energy dissipated by the FRC during the cracking process can be calculated as follows:

$$E_{BCN} = \int_0^{TCOD} P(TCOD)d(TCOD) \quad (3)$$

where E_{BCN} is the energy dissipated up to a given $TCOD$ value. Additionally, according to Molins *et al.* (2009) under these loading conditions, the residual tensile strength of FRC, $f_{ct,Rx}$, can be obtained with the following equation:

$$f_{ct,Rx} = \frac{4\,P_{R,x}}{9\,\pi a H} \tag{4}$$

where $P_{R,x}$ is the load corresponding to a given circumferential deformation R_x, and the dimensions a and H are the diameter of the loading wedge and the height of the cylinder, respectively.

Regarding the control of FRSs used in tunnel support construction, this test has a number of advantages with respect to flexural tests; among them, the test uses relatively small cylindrical test specimens, which can be molded, cut from standard $d = 150$ mm × $h = 300$ mm cylinders or cores drilled from hardened concrete from either filled panels during the spraying process or directly from the hardened support. Moreover, only a conventional compression press is required to execute the test.

In addition, the specimen has a high fracture surface; therefore, the properties of the FRC can be quantified through several fracture planes, which considerably reduces the scatter of the results (Carmona *et al.*, 2012).

4. EQUIVALENCE BETWEEN FLEXURAL AND DOUBLE-PUNCH CRACKING

In the last years, different correlations between 3PB test as the standard EN 14651 and BCN test had been proposed. In this way, Galeote *et al.* (2017) found that the best correlations relate the force measured for a certain value of crack mouths opening displacement ($CMOD$) in the 3PB test with the force and the energy for the same axial displacement measured in the BCN. On the other side Carmona *et al.* (2018) proposed correlations based on crack opening (w). This deformation had been also used by Conforti *et al.* (2017) to correlate 3PB test (EN 14651) and 4PB test (ASTM C 1609).

Then, an equivalence between the 4PB test and the BCN test should be proposed in terms of w; therefore, it is necessary to establish a relationship between the midspan net deflection, δ, recorded in the 4PB test and the crack opening in the beam, $w_{4\mathrm{PB}}$. Then, for a beam with a central crack (Figure 1a), considering the geometric relationships and that $w_{4\mathrm{PB}}$ corresponds to half of the COD measured on the surface of the lower face of the beam, the following relation can be established:

$$w_{4\mathrm{PB}} = \frac{COD}{2} = \frac{2\delta}{3} \tag{5}$$

However, due to the stress state that develops over the central third of the beam in the 4PB test, the location of the cracking plane is random, and the crack rarely opens in the central plane. Considering this factor and the dimensions defined in Figure 2, which shows a beam with an eccentric crack with respect to the central plane, the following relation between COD and net deflection (δ) can be established based on measurements in the center of the length of the beam:

$$w_{4\mathrm{PB}} = \frac{COD}{2} = \frac{2 \cdot \delta \cdot h}{(3h - 2 \cdot e)} \tag{6}$$

where e is the eccentricity of the crack with respect to the central plane of the beam. Equation (6) indicates that the relationship between deflection and the COD is strongly affected by the location of the cracking plane. Therefore, if the crack opens in the center of its length (e = 0), then $COD = 4/3 \cdot \delta$, as is the case in Equation (5), whereas if the crack opens under one of the loading points ($e = L/6$), $COD = 2 \cdot \delta$.

It should be noted that Equation (6) assumes that the crack has propagated through the entire section and that the two parts of the beam rotate around one point, as shown in Figure 2. These assumptions often lead to the overestimation of the COD value. Thus, to obtain more realistic COD values, an analysis can be performed that considers the partially cracked section shown in Figure 3a. In this case, by applying the Bernoulli beam

theory, which assumes a linear strain distribution (Figure 3b) in the cracked section, the following relationship can be proposed for the crack opening w:

$$w = \varepsilon_c \frac{(h-x)^2}{x} = \varepsilon_t (h-x) \quad (7)$$

where ε_c and ε_t are the strains of the most compressed and tensioned fibers of the section, respectively, and h and x are dimensions of the cracked section defined in Figure 3a.

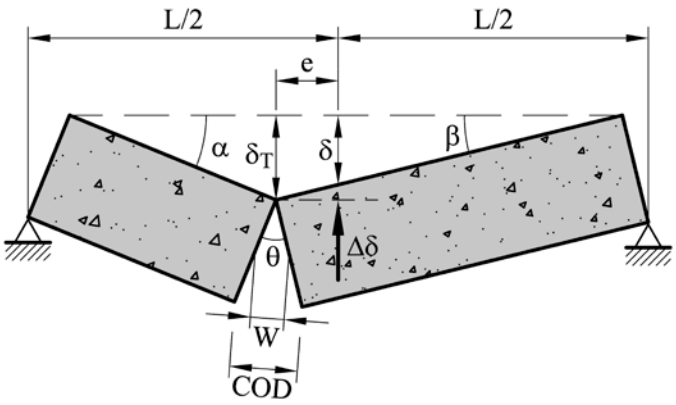

Figure 2. Beam with an eccentric crack.

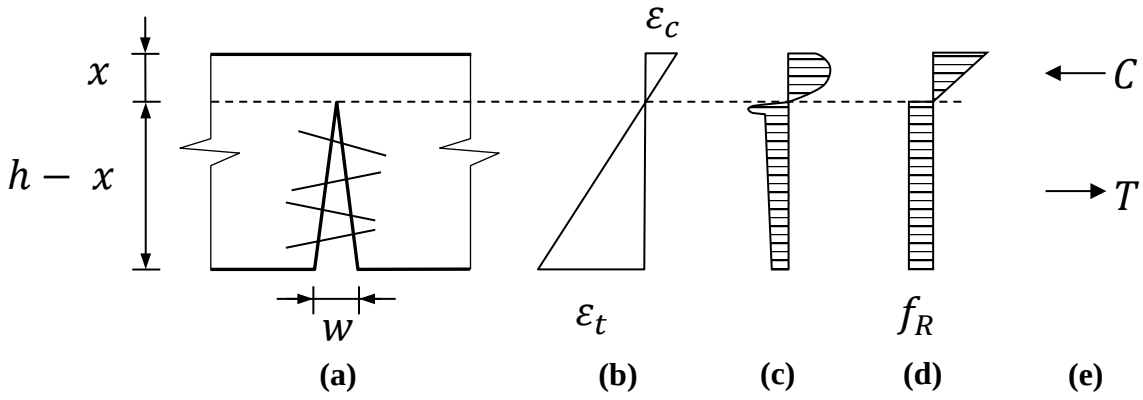

Figure 3. Distributions of strains, real stresses and equivalent stresses in a cracked section of a FRS beam.

Figure 3c shows the complex stress state of the crack with a linear distribution of stresses, as proposed by RILEM TC 162-TDF (2002), or a uniform distribution of tension stresses in the crack, as permitted by the Model Code (CEB-FIP, 2010). This uniform distribution together with the assumption of linear behavior in the non-cracked concrete results in the stress distribution shown in Figure 3d.

By ensuring equilibrium of the internal forces T and C (Figure 3e) and balancing the internal pair with the bending moment produced by external forces, the expressions (8a) and (8b), respectively, are obtained for the strength of the FRC, f_R.

$$f_R = \frac{w \cdot E_c \cdot x^2}{2 \cdot (h-x)^3} \tag{8a}$$

$$f_R = \frac{P \cdot L}{(h-x) \cdot (3h-x) \cdot b} \tag{8b}$$

The modulus of elasticity, E_c, depends on the type of concrete tested, and the nominal values of the specimen dimensions defined in standard C 1609 are h = 150 mm, b = 150 mm and L = 450 mm. Based on the P values obtained experimentally for a given crack opening w, the value of x can be obtained via iterations until both expressions are equal. Because the actual depth of the crack in the section is $h - x$ (Figure 3), the following relationship can be obtained:

$$w_{\text{4PB}} = \frac{COD}{2} = \frac{2\delta(h-x)}{(3h-2e)} \tag{9}$$

Assuming that three radial cracks are produced by the failure mechanism of the FRC cylinder subjected to a DPT, the diameter, $\Delta\phi$, increases. Thus, the average crack opening, w_{BCN}, corresponds to the following equation (Molins *et al*., 2009):

$$w_{\text{BCN}} = \frac{TCOD}{3} \tag{10}$$

Then, equating Equations (9) and (10), the following relationship can be considered:

$$w_{\text{4PB}} = \frac{COD}{2} = \frac{2\delta(h-x)}{(3h-2e)} = w_{\text{BCN}} = \frac{TCOD}{3} \tag{11}$$

This equation relates the mean crack opening with the crack opening displacement and the deflection measured in the 4PB test with the total displacement of the circumferential opening of the cylinder in the BCN test. Therefore, it establishes equivalence between the FRC properties obtained in both tests.

5. EXPERIMENTAL PROGRAM

5.1. Materials

To establish an equivalence between the FRC properties determined with the 4PB and BCN tests, a broad experimental program was developed that included three concretes designed for the inclusion of synthetic fibers. Considering the specification of Chuquicamata Underground Project, the fiber contents used in this research were 6, 8 and 12 kg/m^3. The fiber reinforced concretes were prepared using cement with pozzolanic addition, which was classified as IP-type cement according to the ASTM C 595 standard, and crushed river sand. The mixture details are presented in Table 1. The concretes studied were reinforced with three amounts of synthetic fibers of length l_f = 54 mm, equivalent diameter d_f = 0.84 mm, aspect ratio $\lambda_f = l_f/d_f = 64.3$, tensile strength f_{st} = 640 MPa, modulus of deformation E_f = 12 GPa and 37000 fibers/kg.

Table 1. Mix proportions of tested concretes.

Materials	Doses (kg/m^3)
Cement	420
Total water	215
Sand 0/5 mm	331
Sand 0/10 mm	1324
Plasticizing admixture	2.10
Superplasticizing admixture	2.10
Rheology-controlling admixture	2.94

All the concretes were prepared in a vertical axis mixer to mold the cylinders for the BCN test. For the beams, $H = d$ = 150 mm, i.e., H/d = 1. Standard beams of b = 150 mm × h = 150 mm × l = 530 mm were used in the flexural tests, and three standard cylinders of $d \times h$ = 150 mm × 300 mm were used to determine the compressive strength of each concrete (f_c). The specimens were demolded after 24 hr and remained in a humid chamber until they were tested at approximately 28 days. The number of specimens, the compressive strength and the fiber volume (V_f) for each series are shown in Table 2.

Table 2. Number of significant results and features of concretes of each series used in this research

Concrete	Specimen		f_c (MPa)	Fiber amount (kg/m^3)	V_f (%)
	Cylinder BCN	Beam ASTM			
BC–54–6	10	12	38.6	6	0.66
BC–54–8	9	15	40.9	8	0.88
BC–54–12	10	9	42.3	12	1.32

5.2. Flexural tests

The 4PB tests were performed in a 100-kN capacity servo-hydraulic static system with closed-loop control. To obtain a stable transition between the pre- and post-cracking regime, the tests were performed under COD control. A linear variable differential transducer (LVDT) with a total range of 10 mm was placed at the ends of the central third of the lower face of the beam, as shown in Figure 4. Considering the previously developed relationships between w_{4PB} and δ and to perform the test under conditions like those proposed by standard C - 1609, the elongation of the end fiber pulled from the beam must increase to a ratio between 0.07 and 0.10 mm/min. When the tensile strength of the cement matrix is reached, and the crack opens, this measure corresponds to the COD. During the tests, the load, deflection and COD were recorded at a rate of 3 values/s, and average curves were obtained, as shown in Figure 5.

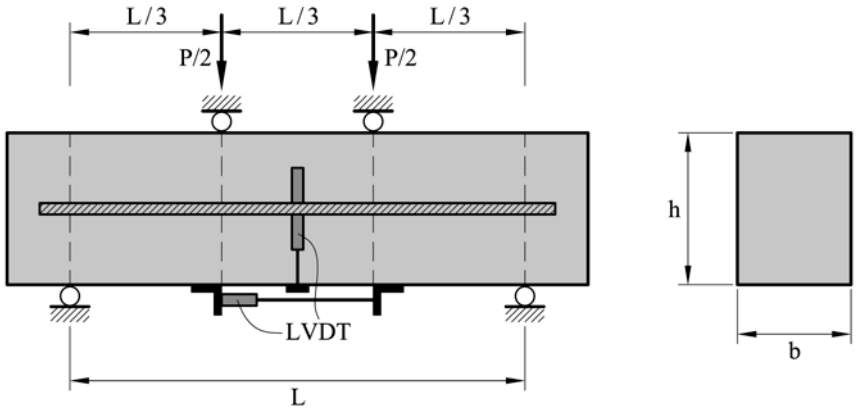

Figure 4. Test set up used for bending tests.

In the average $P-\delta$ curves of Figure 5a, a valley of variable extension is observed after reaching the cracking load based on the quantity of fibers used. In reinforced concrete with 6 kg/m^3 of fibers, a second peak is observed at a deflection of around 1.5 mm with a load on the order of 66% of the average cracking load for that type of FRC; then, the load decreases. In the reinforced concrete with 8 kg/m^3 of fibers, after the valley, the load increases gradually until reaching a peak at a deflection of approximately 2.0 mm, after which the load slowly decreases. Finally, in the case of reinforced concrete with 12 kg/m^3 of fibers, after the valley, the load increases and reaches a second peak at a deflection on the order of 2.0 mm and at a load level like the cracking load.

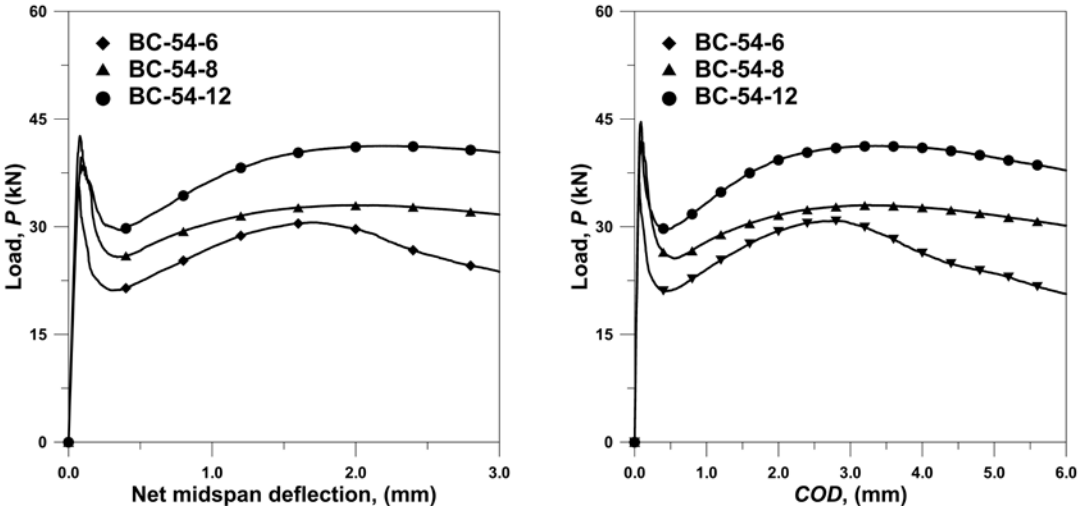

(a) (b)

Figure 5. Average $P-\delta$ and $P-COD$ curves obtained with 4PB tests.

Figure 5b shows the average $P-COD$ curves of each series of concrete studied. The COD values used were obtained from the displacement measured by the LVDT placed under the lower face of the beam, as shown in Figure 4, which were corrected considering the inclination of the LVDT due to the rotation of the beam and the distance from the lower face of the beam to the LVDT axis. These curves exhibit the same behavioral tendencies as those in the $P-\delta$ curves. It should be noted that the curves in Figures 5a and 5b are not plotted until the same time of test, therefore, the curves are not directly comparable.

To determine the relationship between the deflection and the COD, the average $COD - \delta$ curves obtained for each type of FRC tested are plotted, as shown in Figure 6. The curves show that in all the concretes, the relation between $COD - \delta$ is essentially 1:1 until the cracking load is reached for a COD on the order 0.08 mm. After reaching the first peak, the COD increases at a higher rate than deflection, such that for $COD = 6$ mm, the deflection reaches a value on the order of 40% less than the COD. Additionally, the $COD - \delta$ relationship does not appear to depend on the quantity of fibers used.

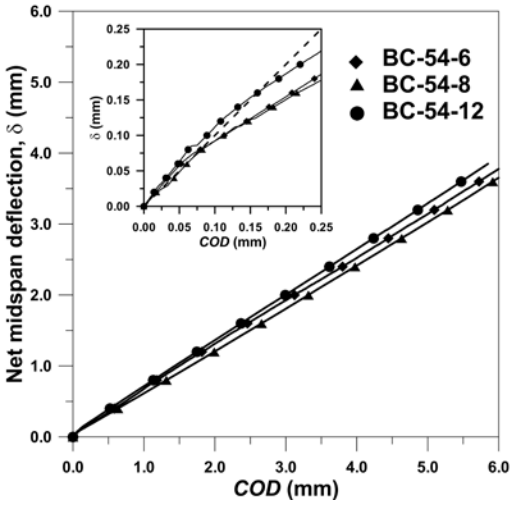

Figure 6. Average $COD - \delta$ curves obtained with FRCs studied.

5.3. BCN tests

BCN tests were performed using the configuration shown in Figure 7a with a 3-MN capacity hydraulic system under displacement control of the actuator at a rate of 0.5 ± 0.05 mm/min. The $TCOD$ was measured with a circumferential extensometer with a total range of 12 mm placed at half the height of the specimen. During the tests, the load, P, and $TCOD$ were recorded continuously at a frequency of 2 data/s, and the average curves for each concrete were obtained, as shown in Figure 7b.

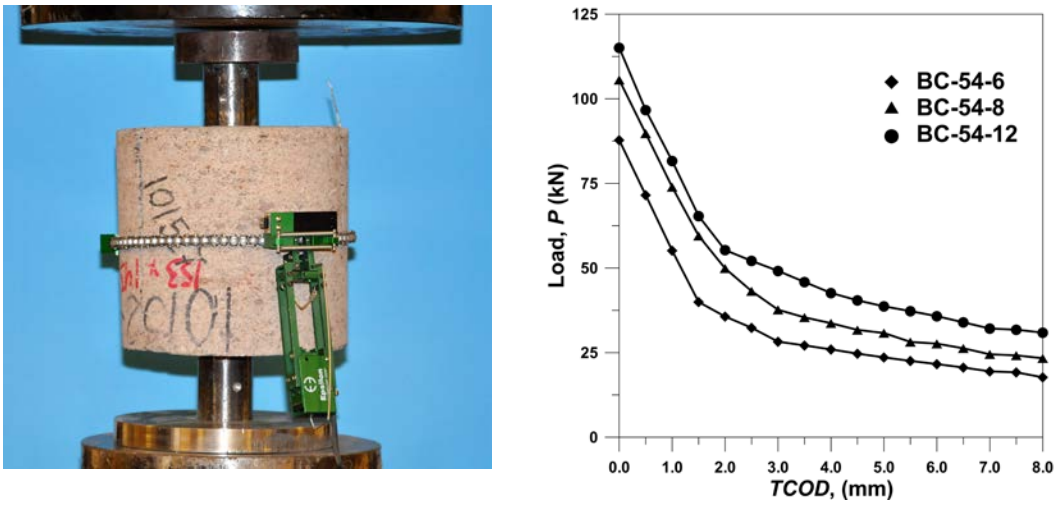

(a) (b)

Figure 7. (a) Setup of BCN test; (b) Average $P - TCOD$ curves obtaine with FRCs tested.

In the curves in Figure 7b, softening is observed after the cracking load is reached, with a strong decrease in the load up to a $TCOD$ of 2.0 mm. Subsequently, a tail can be seen where the load gradually decreases based on the quantity of fibers used.

6. ANALYSIS OF RESULTS

6.1 Relationship between δ and COD

With the deflection records, δ, obtained in the tests and using Equation (5), the crack openings were estimated for each type of FRC, as presented in Figure 8. The actual crack opening was calculated from the COD data collected during each test as $w_{actual} = COD/2$ and is plotted too. As illustrated in the figure, Equation (5) underestimates the crack opening, with an absolute difference with respect to the actual opening of 19.4% for a deflection of 3.0 mm, as shown in Table 3. Additionally, the table indicates that given the proportionality between δ and w_{4PB}, the differences increase with increasing deflection.

Figure 8 also shows the relationship between the deflection and crack opening estimated using Equation (6). In addition to showing the deflection, the figure also illustrates the average width of the crack, as measured on the lower surface of each of the beams tested.

As seen in Table 3, Equation (6) overestimates the crack opening; however, when considering eccentricity in the estimation of $w_{4\mathrm{PB}}$, the difference with the actual crack opening considerably decreases, reaching a maximum of 10.7% for a deflection of 3.0 mm.

Estimates of the crack opening obtained using Equation (9), which, in addition to the eccentricity, includes the depth of the neutral axis, x, calculated with Equations (7) and (8) using the results of each test specimen and the modulus of deformation of the concrete, E_c, of 30676 MPa, are also shown. Based on Figure 8 and the differences presented in Table 3, the values of crack opening estimated with Equation (9) are well adjusted to the values of w_{actual}, with minor differences of less than 2.3%. However, the practical application of this equation requires determining the modulus of deformation of the concrete (E_c) and recording the COD during the test, in which case it would be unnecessary to calculate the value because it would have already been measured.

The differences presented in Table 3 indicate that when the eccentricity of the crack is considered in the estimation of the crack opening, the differences between the estimated values and the actual openings considerably decrease, with a maximum of 10.7% for a deflection of 3.0 mm. In addition, the differences increase as the quantity of fibers used increases.

Because only the $P-\delta$ response and crack eccentricity are determined in the flexure test following ASTM C 1609, the subsequent analyses are performed considering w_{actual} and the estimated values of the crack opening using Equation (6).

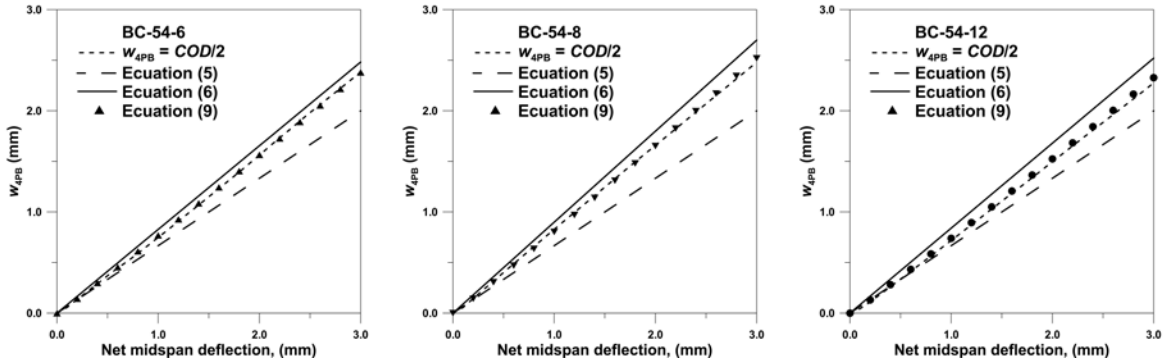

Figure 8. Estimation of the crack opening (w) from the net midspan deflection (δ). ATENCIÓN: Equation NO Ecuation en las leyendas.

Table 3. Percentage differences between the real values of the opening and the estimates using equations (5), (6) and (9).

δ (mm)	BC–54–6			BC–54–8			BC–54–12		
	Eq. (5)	Eq. (6)	Eq. (9)	Eq. (5)	Eq. (6)	Eq. (9)	Eq. (5)	Eq. (6)	Eq. (9)
0.5	-9.9	11.8	2.0	-17.0	11.9	-3.3	-0.9	24.9	6.4
1.0	-10.9	10.6	2.8	-19.5	8.6	-2.9	-7.1	17.1	3.2
1.5	-13.1	7.9	1.3	-19.7	8.3	-1.6	-9.7	13.9	2.1
2.0	-14.6	6.0	0.3	-19.6	8.4	-0.3	-10.9	12.2	1.9
2.5	-15.9	4.3	-0.5	-19.5	8.7	0.8	-11.6	11.4	2.1
3.0	-16.1	4.2	-0.1	-19.4	8.8	1.6	-12.2	10.7	2.3

6.2 Relationship between toughness and dissipated energy

Following the procedure given in ASTM C 1609 and Equation (3), the flexural toughness, T, and the energy dissipated in the BCN test, E_{BCN}, were calculated, respectively, as presented in Table 4. To obtain comparable results in both tests, the values of this table were determined for the same average values of the crack opening, w.

The E_{BCN} values shown in Table 4 correspond to the average crack opening calculated using Equation (10). Additionally, two toughness values for each type of FRC studied are presented. The values in the columns designated T_{actual} are the toughness values calculated at the deflections corresponding to the actual average openings recorded during

the tests and calculated as $w_{4PB} = COD/2$. In the columns designated $T(\delta, e)$, the toughness values were calculated at the deflections corresponding to the average crack openings calculated using Equation (6), and only the eccentricity correction was applied. Because Equation (6) slightly overestimates the values of the mean crack opening with respect to w_{actual}, as shown in Figure 8, the toughness values denominated $T(\delta, e)$ are lower than the T_{actual} values, with differences reaching 28% for small crack openings (w = 0.167 mm) and 10% for crack openings of w = 2.667 mm.

Table 4. Average values of E_{BCN} y T obtained with FRCs tested, in (J).

w (mm)	BC – 54 – 6			BC – 54 – 8			BC – 54 - 12		
	E_{BCN}	T_{actual}	$T(\delta, e)$	E_{BCN}	T_{actual}	$T(\delta, e)$	E_{BCN}	T_{actual}	$T(\delta, e)$
0.167	39.8	5.8	5.0	48.8	7.0	5.8	52.9	8.3	6.0
0.333	71.5	10.4	9.3	89.8	12.1	10.8	97.5	15.0	12.0
0.500	95.1	15.6	13.8	123.1	17.3	15.7	134.3	22.0	18.1
0.667	112.3	21.1	18.7	150.5	22.9	20.9	164.5	29.5	24.6
0.833	127.3	26.8	24.0	173.8	28.8	26.4	191.3	37.5	31.7
1.000	141.6	32.7	29.7	194.0	35.0	32.1	216.6	45.8	39.1
1.167	155.4	38.9	35.6	212.3	41.4	37.9	240.4	54.3	46.7
1.333	168.8	45.1	41.7	229.5	47.9	43.8	262.5	63.0	54.7
1.500	181.4	51.2	47.8	245.9	54.4	49.9	283.3	71.7	62.7
1.667	193.5	57.1	53.9	261.5	61.2	56.0	303.1	80.5	70.9
1.833	205.0	62.6	59.7	276.3	67.9	62.1	322.1	89.3	79.0
2.000	215.9	68.0	65.2	290.2	74.5	68.2	340.3	98.2	87.2
2.167	226.6	73.2	70.4	303.7	81.1	74.3	357.8	107.0	95.4
2.333	236.6	78.4	75.5	316.4	87.7	80.3	374.3	115.5	103.5
2.500	248.1	83.1	80.3	328.6	94.1	86.3	390.2	124.2	111.6
2.667	260.3	88.0	85.0	340.5	100.6	92.2	405.9	132.7	119.5

Figure 9a shows the $E_{BCN} - T_{actual}$ curves obtained for each FRC studied. the plots show that the two properties exhibit a relationship that fits the form given by the following equation:

$$T_{actual} = a_r \, E_{BCN}^{b_r} \tag{12}$$

where a_r and b_r are empirical parameters that depend on the quantity of fibers used. By performing non-linear correlation analysis with the experimental data available, the values of a_r and b_r can be determined, as presented in Table 5, and the fit values are also included in Figure 9a. In the graphs, the obtained curves exhibit a satisfactory fit for advanced cracking states in which the FRC response primarily depends on the reinforcing fibers. However, for values of $w \leq 0.5$ mm, the values estimated with the adjustments of Equation (12) reach differences of up to 58% with respect to the experimental data.

In projects that specify FRS from the properties defined in the ASTM C 1609 standard, the selection of the concrete to be used must be based on the results of flexural tests performed according to the ASTM C 1609 standard on FRS testing, from which the $P - \delta$ responses and crack eccentricities can be obtained. Subsequently, a relationship between $E_{BCN} - T(\delta, e)$ can be established that allows the BCN test to be used to control the work site properties of FRS.

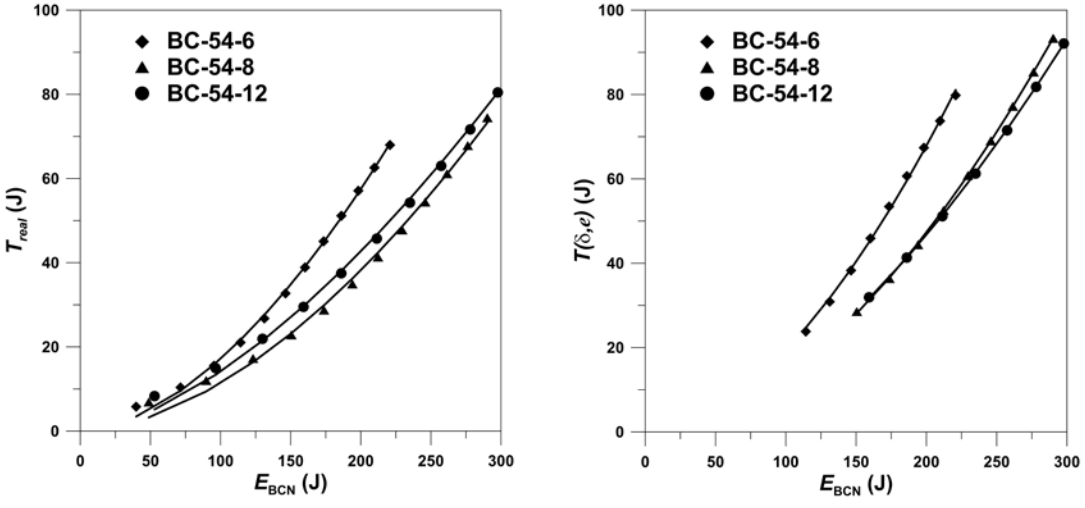

(a) (b)

Figure 9. (a) $E_{BCN} - T_{actual}$ curves; (b) $E_{BCN} - T(\delta, e)$ curves. ATEBCIÓN, ACTUALIZAR TITULO EJE ORDENAS FIGURA (a)

Figure 9b shows the average experimental values of E_{BCN} and $T(\delta, e)$ corresponding to $w > 0.5$ mm. As expected, the graphs in this figure show that the relationship between

toughness and dissipated energy follows the trend given by Equation (12). Analogous to previous methods, a non-linear correlation analysis was performed based on the experimental data, and the values of the empirical parameters a_e and b_e were obtained, as shown in Table 5 and plotted in Figure 9b. The correlations obtained fit the experimental data extremely well.

Table 5. Empirical parameters of equation (12) for the concretes studied.

Concrete	$E_{BCN} - T_{actual}$			$E_{BCN} - T(\delta, e)$		
	a_r	b_r	r^2	a_e	b_e	r^2
BC–54–6	0.0098	1.642	0.9975	0,0059	1.729	0.9959
BC–54–8	0.0025	1,817	0.9981	0,0039	1.724	0.9993
BC–54–12	0.0060	1.664	0.9991	0,0051	1.671	0.9996

Project specifications generally establish requirements based on the toughness calculated at a net midspan deflection of δ = 3.0 mm, T_{150}^{D}. Then, using the experimental results of $T(\delta, e)$ and E_{BCN}, the following expression can be obtained:

$$T_{150}^{D}(E_{BCN}) = 1.60E_{BCN}^{0.7} \quad (13)$$

This fit has a coefficient of determination of r^2 = 0.7935 and allows the BCN test results to be applied to control the toughness based on the dissipated energy E_{BCN}, as determined at a mean crack opening that corresponds to a deflection of $\delta = 3.0$ mm. Table 6 shows that this equation exhibits satisfactory fits for concretes of 6 kg/m^3 and 12 kg/m^3, with an absolute difference of less than 3%. However, the difference is greater for concrete of 8 kg/m^3.

Table 6. Fit of equation (14) to the experimental data.

Concrete	E_{BCN} (J)	T_{150}^{D} (J)	$T_{150}^{D}(E_{BCN})$ (J)	Difference (%)
BC–54–6	236.6	75.5	73.45	-2.7
BC–54–8	316.4	80.3	90.01	12.1
BC–54–12	374.3	103.5	101.24	-2.2

6.3 Relationship between residual strengths f and $f_{ct,Rx}$

With Equations (1) and (3), the residual strengths f and $f_{ct,Rx}$ were calculated using the experimental values obtained in the bending and BCN tests, respectively. Table 7 shows the strength results corresponding to the same crack openings. These values were calculated as previously explained for the analysis of toughness. In this table, two values of the residual bending strength are given: the f_{actual} deflection corresponding to the average actual opening calculated as $w_{4PB} = COD/2$ and f_e calculated at the deflection corresponding to the average crack opening estimated with Equation (6) using δ and e. The values given in Table 7 suggest that the differences between the values of the residual bending strength f_{actual} and f_e are less than 4% for values of $w > 0.5$ mm. Unlike the results of the toughness analysis, these minor differences occur because the residual strength primarily depends on the quantity of fibers and is not proportional to deflection.

Table 7. Residual strengths obtained with BCN and 4PB tests.

w (mm)	BC – 54 – 4			BC – 54 – 6			BC – 54 – 8			BC – 54 - 12		
	$f_{ct.Rx}$	f_{actua}	f_e	$f_{ct.Rx}$	f_{actua}	f_e	$f_{ct.Rx}$	f_{actua}	f_e	$f_{ct.Rx}$	f_{actua}	f_e
0.167	1.95	1.650	2.006	1.75	2.903	3.011	2.26	3.686	3.978	2.37	4.022	4.316
0.333	1.54	1.229	1.292	1.35	2.923	2.865	1.86	3.470	3.439	2.00	4.095	3.962
0.500	1.13	1.199	1.197	0.98	3.214	3.120	1.50	3.713	3.648	1.60	4.436	4.251
0.667	0.77	1.242	1.222	0.87	3.488	3.379	1.25	3.925	3.859	1.35	4.778	4.569
0.833	0.65	1.289	1.271	0.79	3.736	3.628	1.09	4.081	4.020	1.28	5.048	4.853
1.000	0.60	1.327	1.311	0.69	3.918	3.844	0.95	4.206	4.149	1.20	5.241	5.088
1.167	0.55	1.366	1.346	0.66	4.032	3.979	0.89	4.299	4.254	1.12	5.368	5.260
1.333	0.52	1.395	1.378	0.64	4.078	4.064	0.85	4.354	4.325	1.04	5.449	5.372
1.500	0.47	1.414	1.401	0.61	3.994	4.046	0.80	4.386	4.366	0.99	5.488	5.446
1.667	0.44	1.425	1.415	0.58	3.867	3.946	0.77	4.396	4.392	0.95	5.498	5.484
1.833	0.41	1.432	1.426	0.55	3.638	3.749	0.71	4.394	4.395	0.91	5.489	5.498
2.000	0.39	1.433	1.432	0.53	3.466	3.549	0.70	4.363	4.392	0.88	5.455	5.492
2.167	0.37	1.428	1.433	0.50	3.320	3.399	0.66	4.325	4.365	0.83	5.419	5.468
2.333	0.35	1.417	1.429	0.48	3.205	3.270	0.62	4.274	4.327	0.79	5.348	5.432
2.500	0.34	1.403	1.420	0.47	3.088	3.147	0.61	4.224	4.280	0.78	5.280	5.389
2.667	0.33	1.398	1.411	0.43	2.971	3.053	0.59	4.157	4.237	0.76	5.204	5.324

The results presented in Table 7 for values of $w > 0.5$ mm fit an expression of the following form:

$$\frac{f_{actual}}{f_{ct,Rx}} = c(V_f) \cdot w^{d(V_f)} \quad (14)$$

where $c(V_f)$ and $d(V_f)$ are empirical parameters which depend on type and fiber volume, V_f, and they were determined through non-linear regression analysis, obtaining the values given in Table 8 along with the corresponding coefficients of determination, r^2. Nevertheless, these parameters should be determined experimentally for other fiber reinforced concretes.

These values of r^2 indicate a good fit between the parameters and the experimental values, which can be graphically observed in Figure 10. Notably, the differences are less than ± 10% for $w > 1.0$ mm.

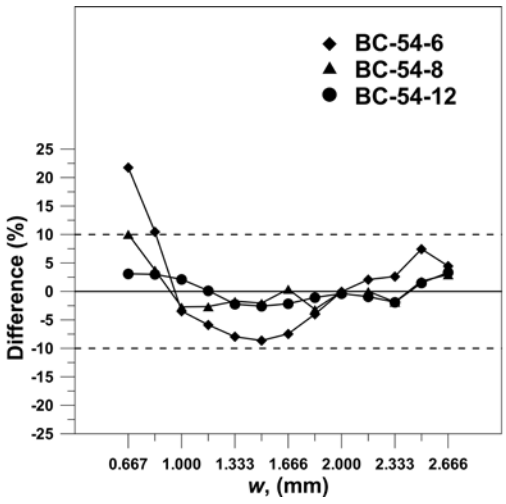

Figure 10. Percentage differences between experimental results and equation (14).

Table 8. Empirical parameters of equation (14) for the concretes studied.

Concrete	$E_{BCN} - T_{actual}$		
	c	d	r^2
BC–54–6	5.362	0.321	0.7893
BC–54–8	4.259	0.567	0.9866
BC–54–12	4.318	0.532	0.9904

Because residual strength f_{150}^{D} is required as the Chuquicamata Underground Project specifications, the following expression was derived:

$$f_{150}^{D}(f_{ct,Rx}) = 7.0 f_{ct,Rx} \quad (15)$$

This equation allows the BCN test results to be applied to control the residual strength based on $f_{ct,Rx}$, which is determined for an average crack opening that corresponds to a deflection of $\delta = 3.0$ mm. As seen in Table 9, this equation exhibits a good fit with the experimental values, with a coefficient of determination r^2 = 0.9870.

Table 9. Fit of equation (15) to the experimental data.

Concrete	$f_{ct,Rx}$ (MPa)	f_{150}^{D} (MPa)	$f_{150}^{D}(f_{ct,Rx})$ MPa	Difference (%)
BC–54–6	0.470	3.164	3.290	3.95
BC–54–8	0.587	4.226	4.110	-2.75
BC–54–12	0.778	5.382	5.449	1.25

VALIDATION OF THE OBTAINED CORRELATIONS

During the construction of the tunnels of the Chuquicamata Underground Project by the mining company CODELCO-Chile, the use of shotcrete reinforced with electro welded steel mesh of $A_s = 295$ mm^2/m and $f_y = 500$ MPa was replaced by sprayed fiber-reinforced concrete with a compressive strength f_c = 30 MPa, a residual strength f_{150}^{D}= 2.15 MPa and an equivalent strength ratio $R_{T,150}^{D} \geq 62\%$ (Carmona, 2012).

FRS testing established that specifications were met by reinforcing shotcrete with 6 kg/m^3 of synthetic fibers. Specifically, 32 beams of 150×150×600 mm were tested. Beams were cut from panels that were filled on site during the spraying of the concrete. In addition, five cores with a diameter of 97 mm and height of 200 mm were cut and tested under compression. An average compressive strength of f_{cm}= 55.4 MPa was obtained.

The beams were tested in a system with closed-loop control under midspan deflection control following the procedure established in the ASTM C 1609 standard. The average

results obtained in the flexural tests are presented in Table 10 with the coefficients of variation (CoV), which are indicated in brackets. As indicated by the CoV, the variability in the results decreased for advanced states of the mean crack opening. Moreover, the flexural toughness has a high CoV, which may originate from the distortions that the $P-\delta$ response exhibits, which are caused by the instability in the transition between the pre- and post-cracking regimes when the first peak is reached in the test, as seen in Figure 11a. Notably, a set of typical $P-\delta$ curves and the average curve obtained in the tests of the studied beams are shown. The CoVs of the BCN test results are lower than those based on the flexural tests.

Table 10. Results of the tests carried out on specimen sampled on-site.

w (mm)	4PB test		BCN test	
	f_{xxx}^{D}	T_{xxx}^{D}	$f_{ct.Rx}$	E_{BCN}
0.167	4.272 (29.9)	2.2 (53.6)	2.061 (12.8)	46.0 (5.7)
0.333	3.824 (33.8)	4.7 (61.6)	1.672 (13.1)	84.1 (7.6)
0.500	3.501 (35.0)	9.5 (46.9)	1.253 (13.5)	114.0 (9.5)
0.667	3.188 (25.5)	15.5 (25.5)	0.839 (13.5)	135.3 (11.5)
0.833	3.318 (25.0)	22.6 (25.5)	0.782 (13.3)	151.9 (12.8)
1.000	3.339 (24.7)	26.4 (27.0)	0.749 (13.5)	167.5 (13.6)
1.167	3.340 (24.8)	30.6 (27.6)	0.718 (13.7)	182.4 (14.2)
1.333	3.363 (24.1)	35.0 (29.3)	0.693 (13.8)	196.8 (14.6)
1.500	3.303 (24.7)	39.2 (29.1)	0.620 (13.9)	210.2 (14.8)
1.667	3.218 (24.4)	43.5 (27.9)	0.550 (13.9)	222.2 (15.0)
1.833	3.202 (22.7)	48.6 (28.2)	0.507 (13.9)	233.0 (15.1)
2.000	3.143 (22.7)	54.1 (28.4)	0.466 (13.9)	242.9 (15.3)
2.167	3.083 (21.5)	58.5 (28.5)	0.440 (14.0)	252.1 (15.4)
2.333	3.000	62.9	0.409	260.8

	(20.4)	(28.7)	(14.1)	(15.6)
2.500	2.912 (20.9)	67.2 (28.8)	0.376 (14.5)	268.8 (14.2)
2.667	2.861 (21.6)	71.5 (28.8)	0.341 (14.6)	276.1 (13.1)

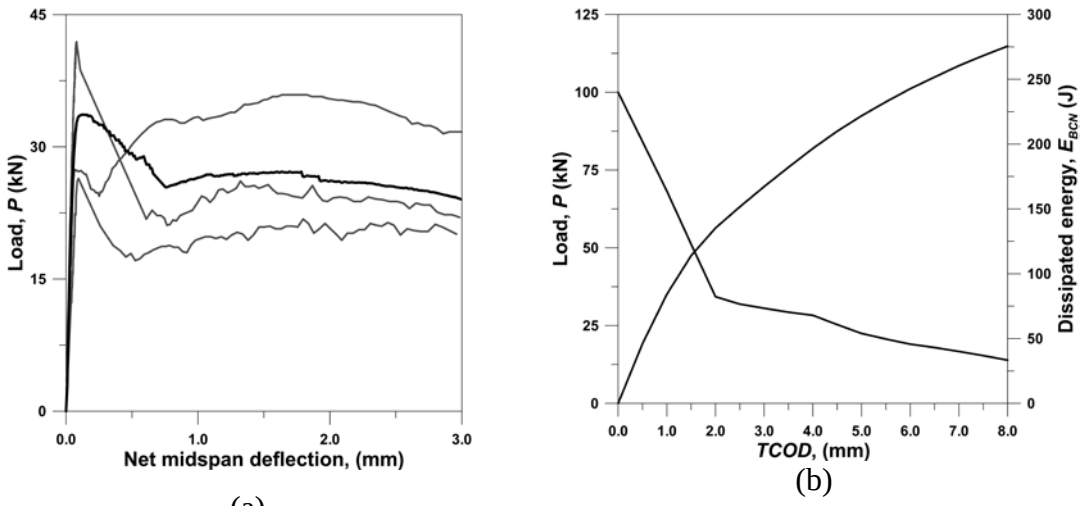

(a) (b)

Figure 11. (a) Typical and average $P-\delta$ curves obtained with 4PB tests carried out on beams sawed from panels sampled on-site; (b) Average $P-TCOD$ curve obtained with BCN tests.

The values given in Table 10 indicate that T_{150}^{D} = 62.9 (J) and f_{150}^{D} = 3.0 MPa. Because the average strength of the first peak obtained in the 4PB tests is f_1 = 4.405 MPa, it can be determined that the equivalent strength ratio of this FRC is $R_{T,150}^{D}$ = 63.1%.

However, the flexural test according to ASTM C 1609 is unsuitable for the on-site control of the properties of fiber-reinforced sprayed concrete due to the difficulty involved in needing to fill panels of at least 200 mm thick on site. Such panels weigh approximately 500 kg and moving them from the excavation site to the laboratory and cutting the beams according to the dimensions specified in the standard is extremely difficult. In addition to these difficulties associated with obtaining samples, the test includes complex inherent steps, such as the need to have a system with closed-loop control to perform the tests. Additionally, instability occurs during the transition between the pre- and post-cracking

regimes when the cracking load is reached, and the deflection measurements exhibit distortion caused by crack eccentricity. These effects have been described in detail in previous sections. Furthermore, the FRS cannot be directly sampled from the tunnel support beams.

Considering the above factors, it was proposed to implement the BCN test for the control of the FRS by testing cores cut from panels or directly from the supports. Of the panels sent to the laboratory, 10 cores of 153 mm in diameter were cut and tested in a 3-MN capacity conventional press used for compression testing following the UNE 83515 standard. The average $P - TCOD$ and $E_{BCN} - TCOD$ curves obtained are shown in Figure 10b, and the results are summarized in Table 10.

Using the eccentricities measured during the tests and Equation (6), it was determined that a net central deflection of δ = 3.0 mm corresponds to a mean crack opening of $w_{4PB} =$ 2.333 mm. In Table 10, for this value of w, the flexural toughness reaches T_{150}^{D}= 62.9 J and the energy dissipated in the BCN test is E_{BCN}= 260.8 J. Replacing this value in Equation (13), $T_{150}^{D}(E_{BCN})$= 78.6 J is obtained. Although this value differs by 25% from the experimentally determined mean value, this difference is smaller than the coefficient of variation of the results, which reaches 28.7%.

In addition, for $w_{4PB} = 2.333$ mm, the average residual strength values are f_{150}^{D} = 3.00 MPa and $f_{ct,Rx}$ = 0.409 MPa. Replacing the last value in Equation (14), $f_{150}^{D}\left(f_{ct,Rx}\right)$ = 2.863 MPa is obtained, which differs by -4.57% from the value determined experimentally. This result reflects the benefits of the correlation obtained with Equation (14), which does not depend on the quantity of fibers or the properties of the cement matrix.

Moreover, this result shows that unlike the correlation obtained for toughness, the residual strength correlation is, according to the presented results, more robust, both for the

laboratory results with different quantities of fibers and for the work site conditions. The differences between the f_{150}^{D} value obtained in the 4PB test and the $f_{150}^{D}\left(f_{ct,Rx}\right)$ value calculated from the BCN test in all cases is less than 5%. This level of 5% is the most common reference used in site control.

The precision of the toughness correlation is clearly lower than that established for the residual strength because it is considerably affected by the initial phase of cracking. Notably, the recorded data show that error is inherent in the deflection measurements because the evolution of the COD cannot be stably controlled by the deflection control mechanism established in the flexural test following ASTM C 1609 standards.

7. CONCLUSIONS

This paper shows that several of the limitations to use the 4PB test for FRCs can be overcome by considering the eccentricity of the actual cracking plane with respect to the central plane. According to ASTM C 1609, this eccentricity is recorded in all the tests, which allows this correction to be easily applied. It is then possible to more realistically estimate the crack opening, which is the fundamental parameter for determining the tensile behavior of fiber-reinforced concrete.

Additionally, both the experimental determinations of test specimens molded in the laboratory and those obtained from drilling the panels manufactured on site indicate that the BCN test exhibits lower dispersion than the 4PB test for a wide range of fiber contents.

A correlation was obtained for the fibers used in this project. This correlation was then used to determine the residual strength f_{150}^{D} from the residual strength of the BCN, and the difference was less than 5% with respect to the values obtained directly from the 4PB test.

The obtained correlations depend on the type of fibers (steel or synthetic), the fiber content and the concrete properties. Then the experimental parameters should be

determined for each specific fiber reinforced shotcrete to be controlled by mean of BCN test.

8. ABBREVIATION

3PB: three-point bending tests.

4PB: four-point bending test or third-point bending test.

BCN test: Barcelona test o double punching test.

COD: crack opening displacement.

DPT: double-punch test.

E_{BCN}: energy dissipated by cylinder under DPT.

f: flexural residual strength.

f_e: flexural residual strength for a $w_{4\mathrm{PB}}$ calculated using equation (6)

f_{actual}: flexural residual strength calculated using equation (1)

f_1: first peak strength.

f_{150}^{D}: flexural residual strength.

$f_{ct,Rx}$: residual tensile strength determined by mean of BCN test.

$R_{T,150}^{D}$: equivalent flexural strength ratio.

$TCOD$: total circumferential opening displacement.

T: flexural toughness.

T_{150}^{D}: flexural toughness at $\delta = L/150$, following ASTM C 1609.

T_{actual}: flexural toughness calculated at δ corresponding a $w_{4\mathrm{PB}}$.

w: crack opening.

$w_{4\mathrm{PB}}$: crack opening in 4PB test calculated using equation (9).

w_{actual}: actual crack opening measured in 4PB test.

w_{BCN}: crack opening in BCN test.

x: depth of the neutral axis on beam.

δ: midspan net deflection.

$T(\delta, e)$: flexural toughness calculated for $w_{4\mathrm{PB}}$.

9. ACKNOWLEDGEMENTS

This research was supported by Fondecyt Project "Use of the Generalized Barcelona Test for Characterization and Quality Control Of Fiber Reinforced Shotcretes In Underground Mining Works", N°1150881.

10. REFERENCES

ASTM International (2012), "ASTM C1609/C1609M-12 Standard Test Method for Flexural Performance of Fiber-Reinforced Concrete (Using Beam with Third-Point Loading)," Annual Book of ASTM Standards, V. 04.02, pp. 9.

Carmona, S. (2012), "Cálculo Reemplazo Malla Acma C – 295 Por Fibra Barchip", 5 pp. (in Spanish).

CEN, (2005) "EN 14651: Test Method for Metallic Fibered Concrete–Measuring the Flexural Tensile Strength (Limit of Proportionality (LOP), Residual)", European Committee for Standardization, Brussels, 2005.

CEN (2006), "EN 14488-5:2006 Testing sprayed concrete. Determination of energy absorption capacity of fibre reinforced slab specimens", 8 pp.

EFNARC (1996), European Specification for Sprayed Concrete. European Federation of National Associations of Specialist Contractors and Material Suppliers for the Construction Industry, 30 pp

Chao, S. H., Karki, N. B., Cho, J. S., Waweru, R. N. (2012), "Use of Double Punch Test to Evaluate the Mechanical Performance of Fiber Reinforced Concrete," In Parra-Montesino, Reinhardt, Naaman, editors. Proceedings of the 6th International Workshop on High Performance Fiber Reinforced Concrete Composites (HPFRCC 6), Ann Arbor, Michigan, pp.27–34.

Carmona, S., Aguado, A., Molins, C. (2012), "Generalization of the Barcelona Test for

the Toughness Control of FRC," Materials and Structures, V. 45, Nº 7, pp. 1053–1069.

Molins C., Aguado A. and Saludes S. (2009), "Double Punch Test to Control the Energy Dissipation in Tension of FRC (Barcelona Test)," Material and Structures, V. 42, pp. 415–425.

AENOR (2010), "UNE 83-515. Hormigones con Fibras. Determinación de la Resistencia a Fisuración, Tenacidad y Resistencia Residual a Tracción. Método Barcelona,". AEN/CTN 83–Hormigón, Madrid, pp. 8 (in Spanish).

Bjøntegaard, Ø., Myren, S.A., Beck. T. (2018), "Quality Control Of Fibre Reinforced Sprayed Concrete: Norwegian Requirements And Experiences From Laboratory Studies And Tunnel Projects", Proceedings of 8th International Symposium On Sprayed Concrete Modern Use Of Wet Mix Sprayed Concrete For Underground Support, Trondheim, Norway, pp. 97–107.

Barragán, B., Gettu, R., Martín, M. A., Zerbino, R. L. (2003), "Uniaxial Tension Test for Steel Fibre Reinforced Concrete – A Parametric Study," *Cement and Concrete Composites.* V. 25, No. 7, pp. 767–777.

Cavalaro, S., and Aguado, A. (2015), "Intrinsic Scatter of FRC: An Alternative Philosophy to Estimate Characteristic Values," *Materials and Structures*, V. 48, No. 11, pp. 3537–3555.

ASTM International (2015), ASTM C 1399/1399M-10 "Standard Test Method for Obtaining Average Residual-Strength of Fiber-Reinforced Concrete" *Annual Book of ASTM Standards*, V. 04.02, pp. 6.

Gopalaratnam, V. S., Gettu, R. (1995) "On the characterization of Flexural Toughness in Fiber Reinforced Concretes", Cement and Concrete Composites, V. 17, pp. 239–254.

Barr, B., Gettu, R., Al-Oraimi, SKA., Bryana, L. S. (1996), "Toughness Measurement - The Need to Think Again". Cement and Concrete Composites, V. 18, pp. 281–297.

Galeote, E., Blanco, A. Cavalaro, S.H.P., De la Fuente, A. (2017), "Correlation between

the Barcelona test and the bending test in fibre reinforced concrete", Construction and Building Materials, V. 152, pp. 529–538. Doi.org/10.1016/j.conbuildmat.2017.07.028.

Carmona, S. Molins, C., Aguado, A., (2018), "Correlation between bending test and Barcelona test to determine FRC properties", Construction and Building Materials, V. 181, pp 673–686. Doi.org/10.1016/j.conbuildmat.2018.05.253.

Conforti, A., Minelli, F., Plizzari, GA., Tiberti, G., (2017) "Comparing test methods for mechanical characterization of fiber reinforced concrete", Structural Concrete, pp. 1- 14. Doi.org/10.1002/suco.20170057.

RILEM TC 162 (2002), "TDF Test and Design Methods for Steel Fibre Reinforced Concrete: Bending Test," *Materials and Structures*, V. 35, pp. 579–582.

CEB-FIP (2010), "Model Code – First Complete Draft," *FIB Bull vol*. 1, V. 55, 2010, pp. 1–318.

ASTM International (2017), "ASTM C 595/C595M–17 Standard Specification for Blended Hydraulic Cements" *Annual Book of ASTM Standards*, V. 04.01, pp. 8.